BMC Microbiology

RESEARCH Open Access

Adoption of an in-silico analysis approach to assess the functional and structural impacts of *rpoB*-encoded protein mutations on *Chlamydia pneumoniae* sensitivity to antibiotics

Sanae Esskhayry[1,2,3,5], Ichrak Benamri[3,4,5], Afaf Lamzouri[1,2], Ouafae Kaissi[2], Rachida Fissoune[3], Ahmed Moussa[3] and Fouzia Radouani[5*]

Abstract

Background Antibiotics are frequently used to treat infections caused by *Chlamydia pneumoniae*; an obligate intracellular gram-negative bacterium commonly associated with respiratory diseases. However, improper or overuse of these drugs has raised concerns about the development of antibiotic resistance, which poses a significant global health challenge. Previous studies have revealed a link between mutations in the *rpoB*-encoded protein of *C. pneumoniae* and antibiotic resistance. This study assessed these mutations via various bioinformatics tools to predict their impact on function, structural stability, antibiotic binding, and, ultimately, their effect on bacterial sensitivity to antibiotics.

Results Eight mutations in the *rpoB*-encoded protein (R421S, F450S, L456I, S454F, D461E, S476F, L478S, and S519Y) are associated with resistance to rifampin and rifalazil. These mutations occur in conserved regions of the protein, leading to decreased stability and affecting essential functional sites of RNA polymerase, the target of these antibiotics. Although the structural differences between the native and mutant proteins are minimal, notable changes in local hydrogen bonding have been observed. Despite similar binding energies, variations in hydrogen bonds and hydrophobic interactions in certain mutants (for instance, D461E for rifalazil and S476F for rifampin) indicate that these changes may diminish ligand affinity and specificity. Furthermore, protein-protein network analysis demonstrated a strong correlation between wild-type *rpoB* and ten *C. pneumoniae* proteins, each fulfilling specific functional roles. Consequently, some of these mutations can reduce the bacterium's sensitivity to rifampin and rifalazil, thereby contributing to antibiotic resistance.

Conclusion The findings of this study indicate that mutations in the *rpoB* gene, which encodes the beta subunit of RNA polymerase, are pivotal in the resistance of *C. pneumoniae* to rifampin and rifalazil. Some of these mutations may

*Correspondence:
Fouzia Radouani
fouzia.radouani@pasteur.ma

Full list of author information is available at the end of the article

result in reduced protein stability and changes in the structure, function, and antibiotic binding. As a consequence, the efficacy of these drugs in inhibiting RNA polymerase is compromised, allowing the bacteria to persist in transcription and replication even in the presence of antibiotics. Overall, these insights enhance our understanding of the resistance mechanisms in *C. pneumoniae* and could guide the development of strategies to address this challenge.

Clinical trial number Not applicable.

Keywords *Chlamydia pneumoniae*, *RpoB* gene, Mutations, In Silico analysis, Antibiotic, Resistance

Background

Chlamydia is a gram-negative, obligate intracellular bacterium that causes various infections in humans and animals [1, 2]. The *Chlamydiaceae* family includes many species, and those pathogenic to humans are *Chlamydia trachomatis* and *Chlamydia pneumoniae*, in addition to several *Candidatus* species [1], as well as the recently described *Chlamydiifrater* genus, *C. phoenicopteri*, and *C. volucris* [3]. *C. pneumoniae* is primarily associated with respiratory tract infections. Untreated or prolonged *C. pneumoniae* infection can lead to several conditions, including lung cancer, Alzheimer's disease, asthma, atherosclerosis, multiple sclerosis, temporal arteritis, stroke, and macular degeneration [4, 5]. The first line of treatment for Chlamydia infections typically involves antibiotics, depending on the specific *Chlamydia* species [5]. However, several factors, such as improper prescription, overuse, or misuse of these drugs, can lead to antibiotic resistance, making treatment ineffective [6, 7]. Antibiotic resistance is a global public health issue that has progressed faster than ever since the discovery of the first antibiotic [8, 9]. Mutations in specific genes are related to the development of antibiotic resistance [5, 7, 10, 11]. In the case of *C. pneumoniae*, mutations in the *rpoB*-encoded protein are linked to resistance to rifampin or rifalazil [11–13]. In silico analysis of gene mutations is a valuable tool that helps enhance experimental research by providing insights into how changes in the genetic code affect the stability, structure, and antibiotic binding. This, in turn, determines the protein's function and the bacterium's sensitivity to antibiotic treatment [14, 15]. While this method has been used to some extent, its application in the study of gene alterations in *C. pneumoniae* is still limited. Notably, Benamri and colleagues reviewed the genes and mutations related to antibiotic resistance in *Chlamydia* species [11]. The study focused on specific mutations in the *rpoB* gene of *C. trachomatis* and *C. pneumoniae* that are associated with resistance to rifamycins, such as rifampin. It also identified mutations in the *gyrA* gene linked to resistance against fluoroquinolones. Additionally, *C. trachomatis* displayed resistance to macrolides (due to mutations in *23 S rRNA*, *rplD*, and *rplV*), tetracyclines (*rpoB*), fosfomycin (*murA*), and MDQA (*secY*). *C. psittaci* demonstrated resistance to aminoglycosides (mutations in *16 S rRNA* and *rpoB*) and macrolides (*23 S rRNA*). On the other hand, *C. suis* exhibited resistance to tetracyclines (*tet(C)*), while *C. caviae* developed resistance to macrolides (*23 S rRNA*). These mutations affect mechanisms such as protein synthesis inhibition and transcription, contributing to antibiotic resistance across different species of *Chlamydia* [11]. Furthermore, they performed an in-silico analysis of *rpoB* mutations to understand their impact on *C. trachomatis* susceptibility to rifamycin [16]. However, despite these significant contributions, a comprehensive understanding of gene mutations and antibiotic resistance across *Chlamydia* species is still relatively lacking, especially in *C. pneumoniae*. In this study, we performed an in-silico analysis of mutant proteins encoded by the *rpoB* gene in *C. pneumoniae* to understand the functional, structural and antibiotic binding impacts of the mutations on the bacterium's resistance to antibiotic treatment.

Methods

In this study, we conducted an in-silico analysis utilizing various bioinformatics tools. Our approach included predicting the functional impact and pathogenicity of genetic variants, assessing changes in thermodynamic stability, analyzing evolutionary conservation, performing structural comparisons of wild-type and mutant models, examining protein-ligand interactions through docking analysis, and investigating protein-protein interactions through network analysis (Fig. 1).

Mutations and native protein sequence retrieval

To identify all *rpoB* gene mutations associated with *C. pneumoniae* antibiotic resistance, we performed a comprehensive literature search targeting databases such as PubMed, ScienceDirect, Google Scholar, and Web of Science, using the following keywords: *Chlamydia pneumoniae*, resistance gene, *rpoB* gene, mutations, antibiotic, and sensitivity to antibiotics. The *C. pneumoniae rpoB*-encoded protein sequence and its 3D structure were obtained from UniProt (https://www.uniprot.org/) and the AlphaFold Protein Structure Database (https://alphafold.ebi.ac.uk/), respectively.

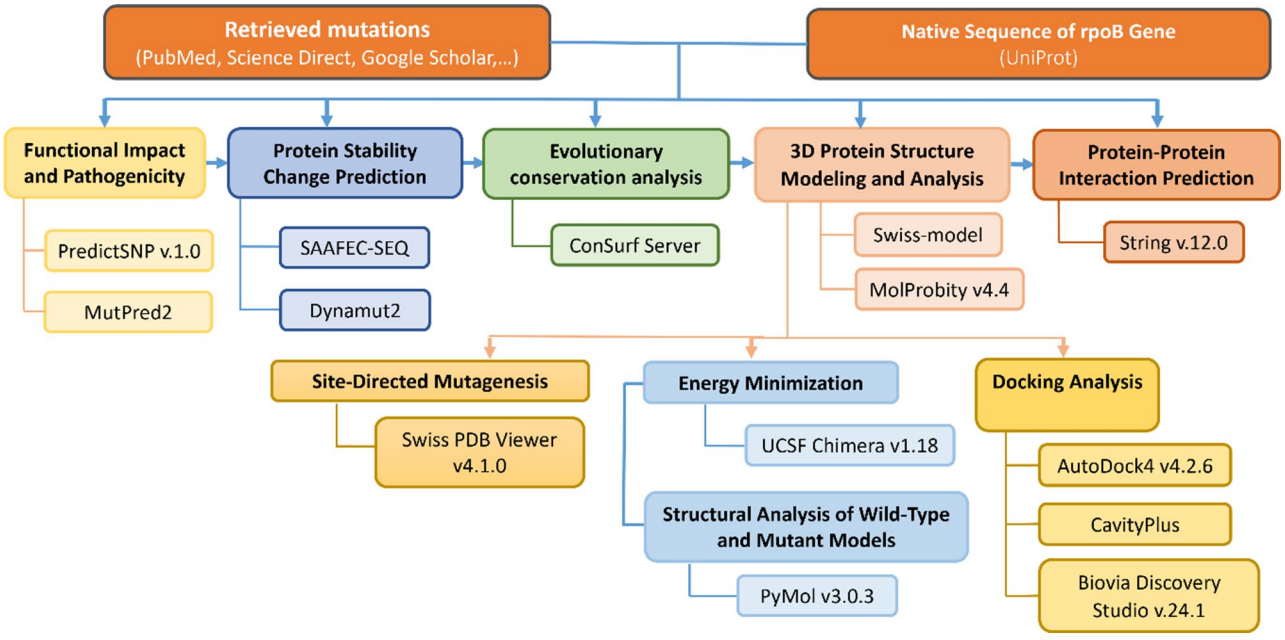

Fig. 1 Study steps fowchart

Functional impact and pathogenicity prediction of variants

To predict the functional impact of amino acid substitutions and their pathogenicity, we used two web-based tools: MutPred2 (http://mutpred.mutdb.org/#qform) [18] and PredictSNP1.0 (https://loschmidt.chemi.muni.cz/predictsnp1/) [19]. MutPred2 is a machine-learning tool that predicts the impact of amino acid substitutions on protein function and pathogenicity. It classifies substitutions as pathogenic or benign, forecasting effects on over 50 protein properties. Integrating genetic and molecular data generates a pathogenicity score from 0 (likely benign) to 1 (likely pathogenic) and identifies affected molecular processes with associated scores [18]. On the other hand, PredictSNP1.0 incorporates nine different bioinformatics tools: SIFT [20], PolyPhen-1 [21], PolyPhen-2 [22], MAPP [23], PhD-SNP [24], SNAP [25], PANTHER [26], PredictSNP [27], and nsSNPAnalyzer [28]. This tool displays the confidence scores from each tool and provides an overall prediction expressed as percentages based on their accuracy levels. We classified mutations as deleterious when the results of five of the nine tools were determined to be deleterious [16].

Prediction of changes in protein thermodynamic stability

Protein stability is crucial for maintaining a protein's structure and function. It is influenced by factors such as amino acid residue interactions, covalent bonds, and environmental conditions such as temperature, pH, and solute concentration [29]. The stability of a protein can be measured by the difference in the Gibbs free energy of unfolding between its native and denatured states ($\Delta\Delta G = \Delta G_{mutant} - \Delta G_{wild-type}$). The sign of $\Delta\Delta G$ determines if a variation increases ($\Delta\Delta G > 0$) or decreases ($\Delta\Delta G < 0$) protein stability [16, 29]. Numerous computational approaches have been developed to predict changes in the thermodynamic stability of proteins due to mutations [30]. This study carefully selected two tools, Dynamut2 (https://biosig.lab.uq.edu.au/dynamut2/submit_prediction_mm) [31] and SAAFEC-SEQ (http://compbio.clemson.edu/SAAFEC-SEQ/index.php#started) [32], to perform this analysis.

Analysis of conserved amino acid residues

The amino acid sequence of a protein provides insight into its structure and function. A comparison of homologous sequences revealed which amino acids are essential for this function. The Consurf server (https://consurf.tau.ac.il) was utilized to identify the locations of amino acids based on evolutionary conservation [33–35]. The conservation scores range from 1 to 9, with 1 being the least conserved region and 9 being the most conserved region.

Site-directed mutagenesis analysis

Hydrogen bonds play a crucial role in stabilizing protein structures and influencing their functional properties. Therefore, understanding how mutations affect hydrogen bonding is essential for evaluating their impact on protein function [36]. In this study, we introduced site-directed mutations in the *rpoB*-encoded protein using Swiss PDB Viewer software version 4.1.0 [37]. This allowed us to transform the 3D structure from its native form into mutant forms, enabling us to examine the

hydrogen bonding patterns in both the native and mutant structures of the protein.

Protein 3D mutant structure modeling and validation

To evaluate the impact of each mutation on protein structure, we constructed 3D models of the mutant proteins encoded by *rpoB* gene using SWISS-MODEL (https://swissmodel.expasy.org/) [38]. This tool employs a homology modeling algorithm to generate 3D structures based on sequence alignment with established templates. We chose the model of highest quality based on sequence identity and the Global Model Quality Estimation (GMQE) [38]. To verify the reliability of the models, we created Ramachandran plots using MolProbity version 4.4 [39]. Following the modeling process, we conducted energy minimization with UCSF Chimera v.1.18 using the steepest descent algorithm [40, 41]. This step optimizes the molecular arrangement by minimizing steric clashes and achieving a more stable, energetically favorable conformation.

Comparison of the structures of wild-type and mutant models

We compared the structures of the native and mutated proteins by calculating the Root-Mean-Square Deviation (RMSD) between the wild-type and mutated structures using PyMol software version 3.0.3. A smaller RMSD value indicates a greater structural similarity [42].

Molecular docking analysis

To understand how structural changes resulting from mutations can affect antibiotic sensitivity, we conducted a molecular docking analysis using AutoDock4 (version 4.2.6) [43–45]. This analysis simulates the binding of antibiotics to both wild-type and mutant protein structures, allowing us to predict how mutations may alter binding affinity. We determined the grid box coordinates and dimensions in the x, y, and z directions using CavityPlus 2022 (http://www.pkumdl.cn:8000/cavityplus#/) tool with ligand mode whenever possible [46]. Additionally, we utilized BIOVIA Discovery Studio v.24.1 to create 2D visualizations that highlight key aspects of the protein-ligand interactions [47].

Table 1 *rpoB*-encoded protein mutations related to antibiotic resistance in *C. pneumoniae*

Study	Reference	Antibiotic	Mutation
Kutlin et al. 2004	[12]	Rifampin	L456I
		Rifalazil	D461E
Rothstein et al. 2008	[13]	Rifampin	S454F
			L478S
			F450S
			R421S
			S519Y
			L456I
			S476F

Prediction of protein-protein interactions

To investigate the interaction of the *rpoB*-encoded protein with various proteins, the STRING server (version 12.0) (https://string-db.org) [48] was used. This allowed us to contextualize the *rpoB* gene within its broader protein interaction network, helping to explore its functional relationships with other proteins within the *C. pneumonia* system [48, 49].

Results

Retrieved and collected data

A literature search revealed eight mutations in the *rpoB*-encoded protein related to the antibiotic resistance of *C. pneumoniae* to rifampin or rifalazil. These mutations were identified in studies by Kutlin et al. in 2004 [12] and Rothstein et al. in 2008 [13] (Table 1). The sequence data for the wild-type *rpoB*-encoded protein were obtained in FASTA format from the UniProt database (UniProt ID: Q9Z9A0). The predicted 3D structure was retrieved from the AlphaFold database (AlphaFold DB: AF-Q9Z9A0-F1, https://alphafold.ebi.ac.uk/search/text/AF-Q9Z9A0-F1), with an average quality score (pLDDT) of 88.5. This score indicates that the predicted 3D structure of the wild-type protein is of high quality.

Functional impact of variants and their pathogenicity

The eight mutations previously collected were analysed with both MutPred2 and PredictSNP1.0 tools. Pathogenic mutations (R421S, F450S, S454F, D461E, S476F, L478S, and S519Y) consistently show harmful predictions across both tools (Table 2), leading to alterations in critical motifs and multiple molecular modifications that disrupt protein structure and function (Table 3). The benign mutation L456I (MutPred2 score < 0.5), despite being predicted to be deleterious by PredictSNP1.0, shows no affected motifs or molecular alterations. Similarly, although the D461E mutation is expected to be harmful, it does not involve modifications to specific molecular mechanisms.

Prediction of changes in protein thermodynamic stability

The prediction of changes in protein stability for the eight mutations within the *rpoB*-encoded protein was conducted via two distinct tools, SAAFECSEQ and Dynamut2. The mutations were predicted to decrease the stability of the *rpoB*-encoded protein in *C. pneumoniae* strains ($\Delta\Delta G < 0$) (Fig. 2).

Analysis of conserved amino acid residues

The Consurf tool results suggest that the *rpoB*-encoded protein's specific residues are conserved. Each of the 8

Table 2 Prediction of the functional impact and the pathogenicity of variants via the MutPred2 and PredictSNP1.0 tools

Amino acid change	MutPred2			PredictSNP1.0
	Score	Prediction	Affected PROSITE and ELM Motifs	Prediction
R421S	0.892	P	ELME000062, ELME000233.	D
F450S	0.853	P	ELME000053,ELME000146, ELME000336.	D
S454F	0.631	P	ELME000063,ELME000202,ELME000328, ELME000336.	D
L456I	0.384	B	ND	D
D461E	0.592	P	ELME000052, ELME000336	D
S476F	0.876	P	ELME000008,ELME000062, ELME000085, ELME000106 ,ELME000146,ELME000249, ELME000334, PS00004.	D
L478S	0.854	P	ELME000008,ELME000062,ELME000085, ELME000336.	D
S519Y	0.919	P	ELME000053,ELME000063,ELME000182, ELME000333, ELME000336, PS00008.	D

B: refers to the benign variant, **D**: refers to the deleterious/nonstable effect, **P**: stands for the pathogenic variant, and **ND**: Not Determined

Table 3 Results of the molecular mechanism predictions of amino acid substitutions via MutPred2

Amino acid change	Molecular mechanisms with *P* values < = 0.05 (Probability)		
	Loss	Gain	Altered
R421S	Allosteric site at R421 (0.37), Helix (0.27).	Proteolytic cleavage at D426 (0.11).	DNA binding (0.22), Metal-binding (0.14), Disordered interface (0.29), Coiled-coil (0.10).
F450S	ND	Intrinsic disorder (0.32), Methylation at K448 (0.10).	Disordered interface (0.28), Stability (0.12).
S454F	ND	ND	Disordered interface (0.33), Ordered interface (0.33).
S476F	Methylation at K472 (0.12).	Allosteric site at R474 (0.33), Catalytic site at R474 (0.10).	DNA binding (0.19), Metal-binding (0.14).
L478S	Allosteric site at R474 (0.25).	Relative solvent accessibility (0.27), B-factor (0.26), Intrinsic disorder (0.42), Catalytic site at G479 (0.12).	Metal binding (0.14), DNA binding (0.18), Stability (0.26), Ordered interface (0.31).
S519Y	Catalytic site at S519 (0.17).	Allosteric site at S519 (0.36).	Metal binding (0.31), Ordered interface (0.28), DNA binding (0.23), Transmembrane protein (0.15).

ND: Not Determined

residues had a high conservation score (9). More specifically, 3 positions were located on surface-exposed residues (F), and 5 positions were buried within the protein (S) (Table 4).

Site-directed mutagenesis results

Using Swiss PDB Viewer version 4.1.0, we converted the 3D structure of the *rpoB*-encoded protein from its native form to its mutant form. The Comparison of the native and mutant structures (Fig. 3a and b) revealed significant changes in the positioning of hydrogen bonds.

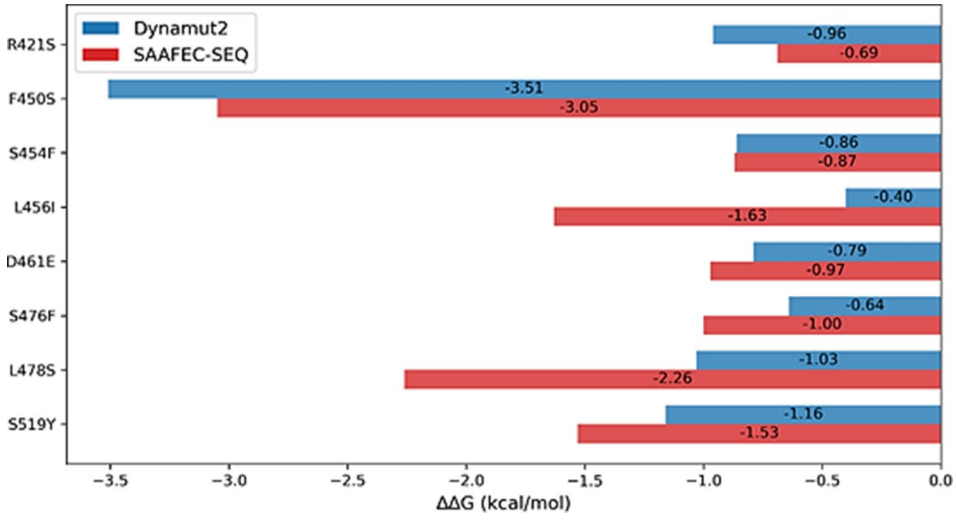

Fig. 2 Prediction of changes in protein stability via the SAAFECSEQ and Dynamut2 tools

Table 4 Evolutionary conservation analysis of amino acids in the *RpoB* gene-encoded protein

Amino acid change	Conservation score	Prediction
R421S	9	Highly conserved and exposed (F)
F450S	9	Highly conserved and buried (S)
S454F	9	Highly conserved and exposed (F)
L456I	9	Highly conserved and buried (S)
D461E	9	Highly conserved and exposed (F)
S476F	9	Highly conserved and buried (S)
L478S	9	Highly conserved and buried (S)
S519Y	9	Highly conserved and buried (S)

3D modeling of mutant proteins and validation

All mutant models were generated using the SWISS-MODEL, achieving a sequence identity of 79.55% with the template and a GMQE score of 0.89, indicating high confidence in the reliability and quality of the predicted 3D structures (Table 5). The Ramachandran favorable region percentages are consistently high, ranging from 96.14 to 97.35%, reflecting well-optimized structural geometries (Fig. 4).

Table 5 Assessment of the structure of 3D models of mutant proteins generated by SWISS-MODEL

Amino acid change	Sequence Identity	GMQE	Ramachandran favourable region (%)
R421S	79.55%	0.89	96.14%
F450S	79.55%	0.89	96.14%
S454F	79.55%	0.89	97.35%
L456I	79.55%	0.89	96.31%
D461E	79.55%	0.89	96.14%
S476F	79.55%	0.89	96.31%
L478S	79.55%	0.89	96.14%
S519Y	79.55%	0.89	97.27%

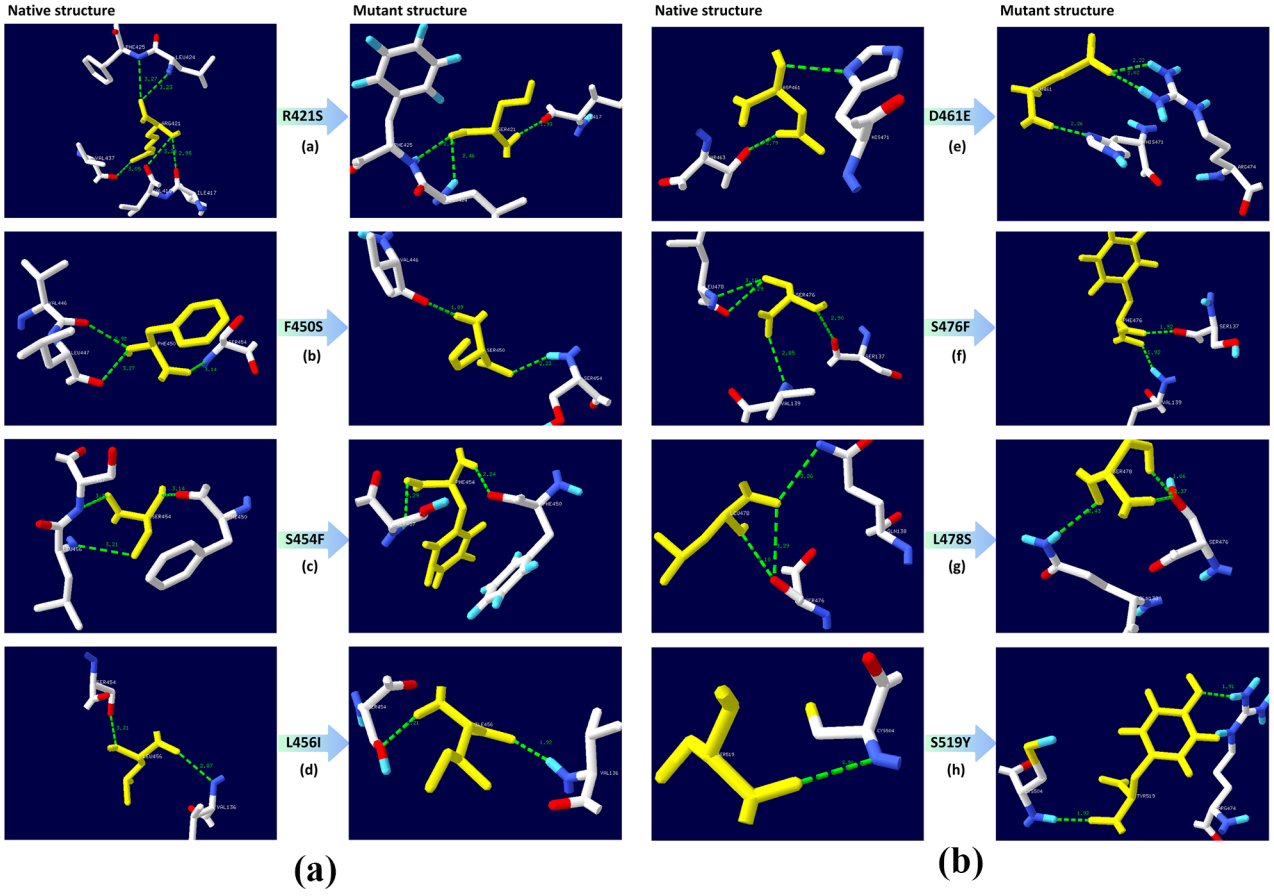

Fig. 3 **[a]** Comparison of *rpoB*-encoded protein hydrogen bonding, from the native to the mutant structure. **a** Wild type R and mutant S residues at 421th position (R421S). **b** Wild type F and mutant S residues at 450th position (F450S). **c** Wild type S and mutant F residues at 454th position (S454F). **d** Wild type L and mutant I residues at 456th position (L456I). **[b]** Comparison of Hydrogen Bonding in the rpoB-Encoded Protein Between the Native and Mutant Structures. **e** Wild type D and mutant E residues at 461th position (D461E). **f** Wild type S and mutant F residues at 476th position (S4767). **g** Wild type L and mutant S residues at 478th position (L478S). **h** Wild type S and mutant Y residues at 519th position (S519Y)

Structural comparison between mutant and wild-type proteins

To evaluate the structural impact of mutations, we superimposed the 3D structures of the native and mutant forms of the *rpoB*-encoded protein (Fig. 5). The analysis revealed minimal structural deviations, with RMSD values ranging from 0.022 Å to 0.024 Å for all the studied mutations (Table 6).

Binding site alterations analysis

The analysis of the binding sites for both the wild-type and mutant forms revealed significant reductions in binding pocket volume and surface area across all mutants compared to the wild-type. The wild-type protein had a larger pocket volume of 7940.62 $Å^3$ and a surface area of 2553.50 $Å^2$. In contrast, the mutants consistently exhibited reduced volumes, ranging from 5830.62 $Å^3$ to

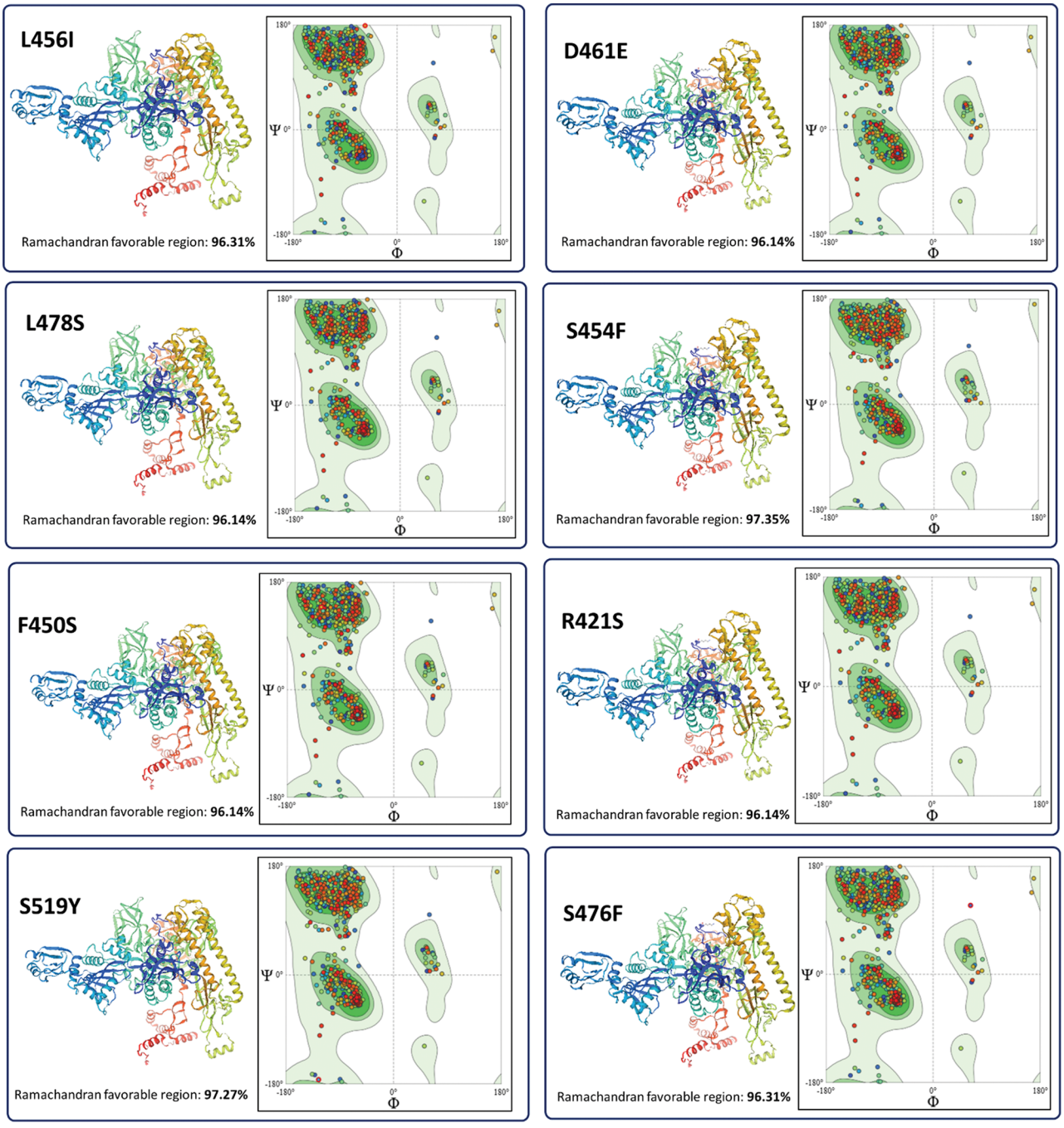

Fig. 4 Three-dimensional structures of the predicted mutant proteins, along with Ramachandran favorable regions and corresponding plots generated by MolProbity

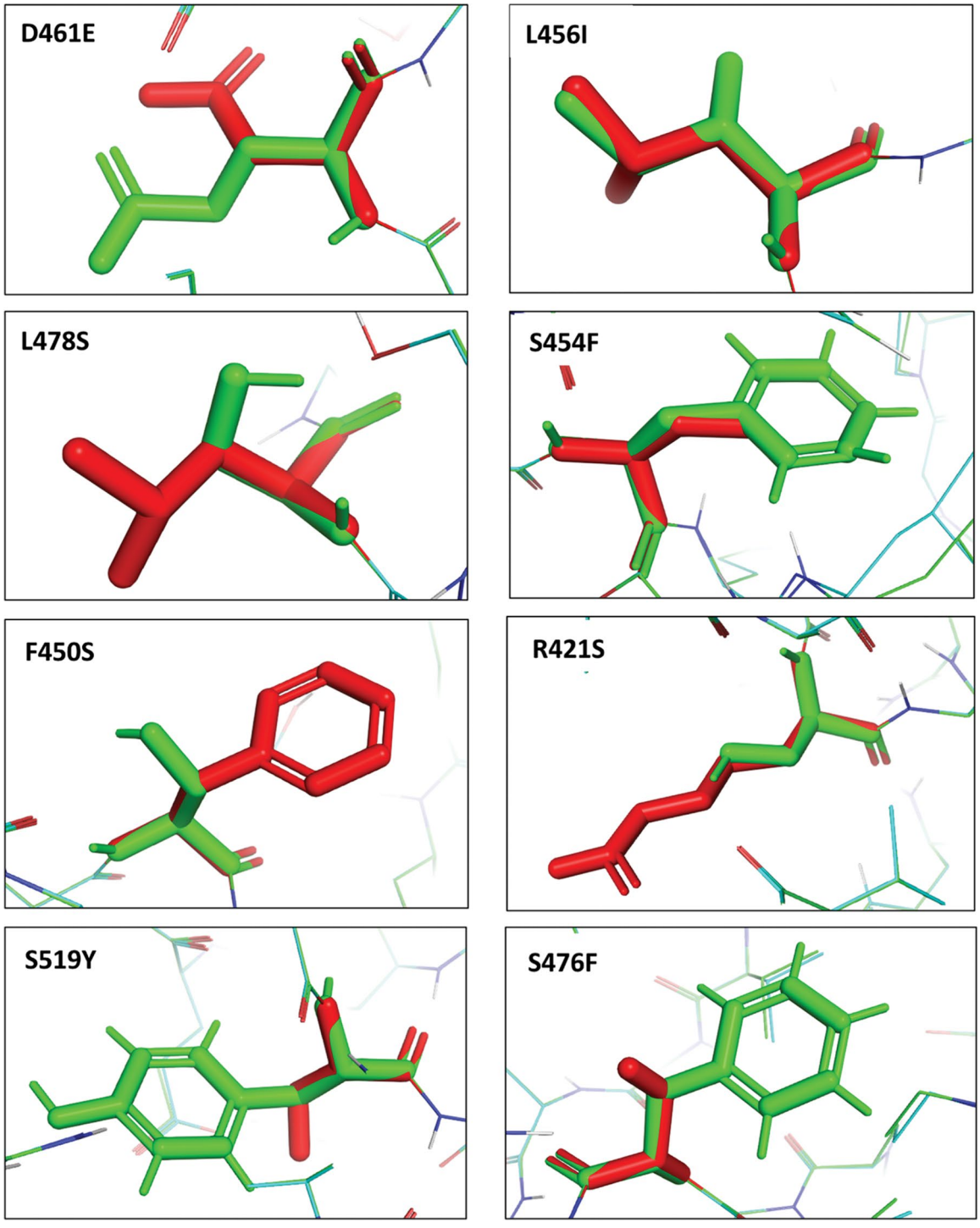

Fig. 5 The superimposed structures of the mutant and wild-type amino acids of the *rpoB*-encoded protein at different positions. The native amino acid is red, and the mutant amino acid is green

5905.62 Å^3, with surface areas approximately between 1885 Å^2 and 1896 Å^2 (Table 7).

Molecular docking results

The docking results indicate that the binding energies for both the wild-type and mutant proteins are comparable. Notably, rifalazil shows a slightly stronger binding affinity in the wild-type (-10.56 kcal/mol) compared to rifampin (-9.79 kcal/mol) (Fig. 6). Mutants such as D461E, F450S, and R421S exhibit binding energies similar to those of the wild-type, while others, including S476F and L478S, demonstrate marginally weaker binding affinities (Fig. 6).

Table 6 RMSD values of the *rpoB*-encoded protein between the native and mutant structures

Amino acid change	RMSD (Å)
R421S	0.024
F450S	0.024
S454F	0.022
L456I	0.024
D461E	0.024
S476F	0.023
L478S	0.024
S519Y	0.023

Table 7 Binding site properties of wild-type and mutant *rpoB*-encoded proteins predicted by CavityPlus

Amino acid change	Box Size (Å)	Box Center (Å)	Volume ($Å^3$)	Surface Area ($Å^2$)
Wild type	29.0 32.0 31.0	-11.5 10.0 6.5	7940.62	2553.50
R421S	26.5 28.5 23.5	-12.75 11.25 9.75	5858.12	1888.00
F450S	26.5 28.5 23.5	-12.75 11.25 9.75	5858.12	1888.00
S454F	26.5 28.5 23.5	-12.75 11.25 9.75	5860.75	1885.75
L456I	26.5 28.5 23.5	-12.75 11.25 9.75	5858.25	1887.75
D461E	26.5 28.5 23.5	-12.75 11.25 9.75	5830.62	1886.25
S476F	26.5 28.5 23.5	-12.75 11.25 9.75	5905.62	1896.00
L478S	26.5 28.5 23.5	-12.75 11.25 9.75	5858.25	1887.75
S519Y	26.5 28.5 23.5	-12.75 11.25 9.75	5857.25	1885.25

Mutations significantly alter the interaction patterns of both rifalazil and rifampin compared to the wild-type protein (Table 8). In the wild-type, rifalazil forms a strong binding interaction through a hydrogen bond with ASN:45 and has extensive hydrophobic interactions with residues such as ILE:46 and GLU:528 (Table 8). In contrast, rifampin forms a single hydrogen bond with SER:398 and has fewer hydrophobic interactions. When mutations occur, rifalazil completely loses its hydrogen bonding (e.g., in D461E), with its interactions shifting solely to hydrophobic contacts involving residues like TYR:166 and LYS:28 (Table 8). For rifampin, mutations such as F450S and R421S enhance hydrogen bonding (e.g., with ASN:45 and ARG:337), increasing its polar interactions. However, in other mutants, such as S476F and L456I, rifampin loses its native hydrogen bonds and relies heavily on hydrophobic interactions with residues like ILE:36 and VAL:76 (Table 8).

While the binding energies remain similar across different protein variants, the distinct patterns of interactions, particularly regarding hydrogen bonds and hydrophobic contacts, suggest that these variations may influence the ligand's affinity and specificity (Figs. 7 and 8).

Protein-protein interactions

Analysis of protein-protein interactions has revealed insights into the activities and connections of several important proteins in the bacteria *C. pneumoniae* (Fig. 9). The protein encoded by the *rpoB* gene interacts with

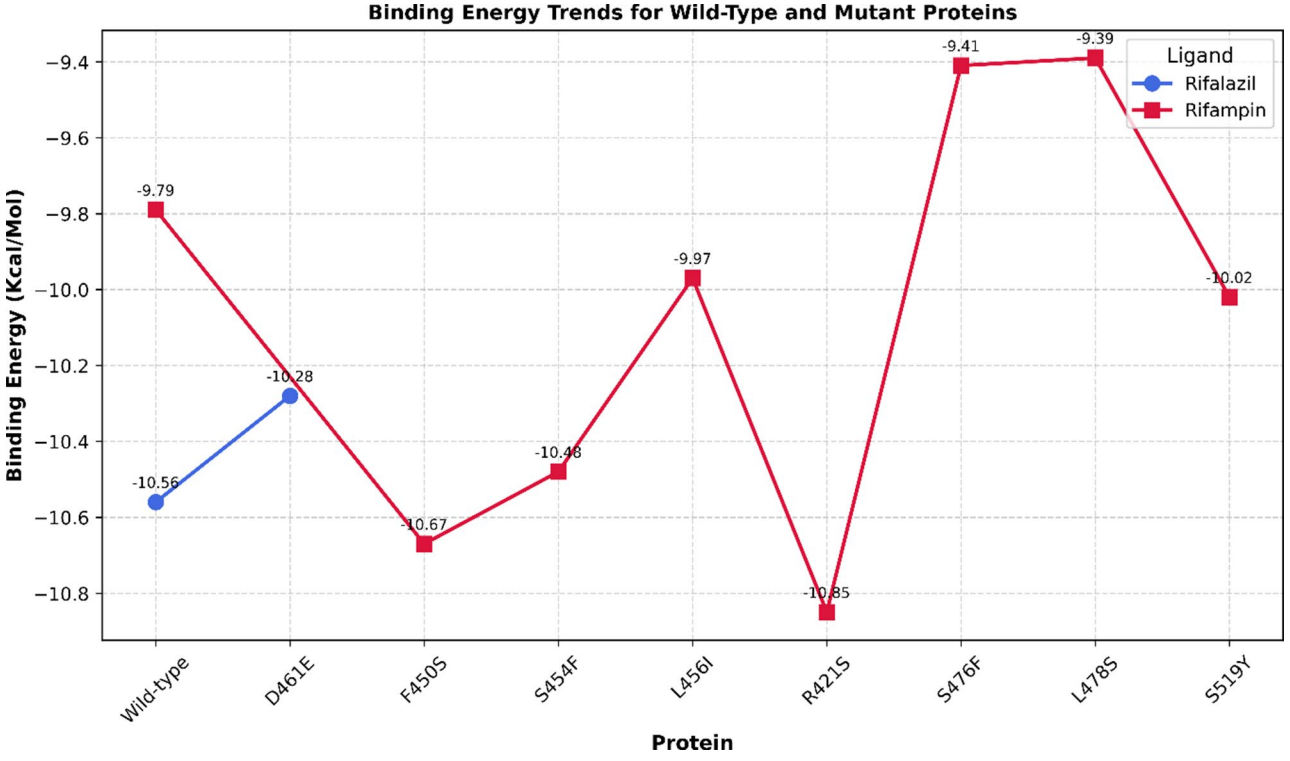

Fig. 6 Binding energy (Kcal /Mol) trends for wild-type and mutant proteins

Table 8 Docking analysis of wild-type and mutant *rpoB* proteins withrifalazil and rifampin: interactions involving conventional hydrogen bonds and hydrophobic interactions (Pi-Sigma & Pi-Alkyl, alkyl and Amide-Pi Stacked)

Protein	Ligand	Interactions	
		Conventional Hydrogen bond	Hydrophobic (Pi-Sigma & Pi-Alkyl, alkyl and Amide-Pi Stacked)
Wild-type	Rifalazil	ASN:45	ILE:46, GLU:528, ILE:526, LYS:28, ILE:25, LYS:525, PRO:20
	Rifampin	SER:398	ILE:25, ILE:526
D461E	Rifalazil	-	TYR:166, ILE:46, LYS:525, LYS:28
F450S	Rifampin	ASN:45, ASN:334, VAL:338, ARG:337	ILE:46
S454F	Rifampin	VAL:338, ARG:337, ASN:334, ASN:45	ILE:46
L456I	Rifampin	-	ILE:36, THR:981, LEU:74, VAL:76, ARG:985
R421S	Rifampin	VAL:338, ARG:337, ASN:334, ASN:45	ILE:46
S476F	Rifampin	LEU:39	ILE:36, VAL:76, VAL:93, PRO:77, LEU:119
L478S	Rifampin	LEU:39	ILE:36, LEU:119, PRO:77, VAL:76
S519Y	Rifampin	THR:690	ILE:687

various proteins, including RpoC, RpoA, RpIK, RpIF, RpIC, RpIV, RpIJ, RpsE, RpIL, and RpsC, as indicated by the scores (Table 9). Each protein has a unique function that is crucial for cellular activities such as transcription and translation. These interactions are supported by high confidence values, highlighting their reliability.

Discussion

C. pneumoniae is a pathogenic bacteria known for causing respiratory tract infections [4, 5]. Antibiotics that target DNA and protein synthesis, such as macrolides, tetracyclines, and quinolones, are effective against *C. pneumoniae* [4, 50–52]. However, with the overuse or misuse of these drugs, this bacterium can develop resistance to specific antibiotics through different mechanisms [6, 10, 53–55]. Mutations in the *rpoB*-encoded protein of *C. pneumoniae* are associated with resistance to rifampin and rifalazil antibiotics [11–13]. these drugs inhibit bacterial RNA polymerase by binding to its beta-subunit, disrupting RNA synthesis which is critical for bacterial survival [5]. These mutations can alter the protein's structure, stability, and antibiotic binding, thereby impacting its function and the bacterial response to antibiotics. To investigate these effects, we conducted an in-silico analysis using bioinformatics tools to evaluate the structural and functional implications of these mutations. Each tool provides a different perspective—functional, evolutionary, structural, or interaction-based—regarding how a mutation could influence protein behavior and its subsequent role in bacterial sensitivity to antibiotics. The deleterious effects of the eight identified mutations (Table 1) were predicted via PredictSNP 1.0 [19]. The analysis revealed that all mutations in the *rpoB*-encoded protein are predicted to be deleterious (Table 2). Using the MutPred2 tool, mutations R421S, F450S, S454F, S476F, L478S, and S519Y were identified as potentially affecting critical functional sites. These sites include those involved in DNA binding, metal binding, and catalytic activity, which may compromise the effectiveness of RNA polymerase— the target for various antibiotics (Table 3). As a result, these alterations could diminish the efficacy of antibiotics and contribute to resistance by obstructing their ability to bind to target proteins. The benign mutation L456I has minimal functional impact with no affected motifs or molecular alterations, as shown in Tables 2 and 3, despite being predicted as deleterious by PredictSNP1.0. Similarly, the D461E mutation was also predicted to be pathogenic across different tools, and lacks affected motifs (Table 2) and specific molecular mechanism alterations (Table 3), suggesting a potentially less severe impact. The discrepancies in the results highlight the need for deeper predictions via new tools. The results from the Consurf server [33–35] show that the specific residues of the mutant proteins are conserved, with conservation scores equal to 9 (Table 4). Mutations in these areas can significantly affect the function and stability of the protein, potentially leading to misfolding or loss of function. These areas typically encompass active sites, binding sites, or interaction domains crucial for protein activity. This, in turn, could lead to drug resistance or altered drug efficacy. On the other hand, the use of Dynamut2 [31] and SAAFECSEQ [32] to predict alterations in protein thermodynamic stability revealed negative values of the difference in the Gibbs free energy of unfolding (Fig. 2), indicating that the mutations would likely disrupt the protein structure, potentially resulting in misfolding degradation or abnormal protein aggregation. The predicted three-dimensional structures of the mutant proteins, validated through Ramachandran plots, demonstrate their reliability, with over 90% of residues situated in favored regions (Table 5) and (Fig. 4). The minimal RMSD values, ranging from 0.022 to 0.024 Å, indicating that the mutations do not significantly affect the overall architecture of the protein. However, these mutations disrupt or modify crucial hydrogen bonding patterns that are essential for the binding and stability of the protein (Fig. 3. a and b). Although the global structure of the protein remains intact, these localized changes are likely to diminish ligand efficacy, underscoring the impact of specific amino acid substitutions on the development of antibiotic resistance [36]. The docking results

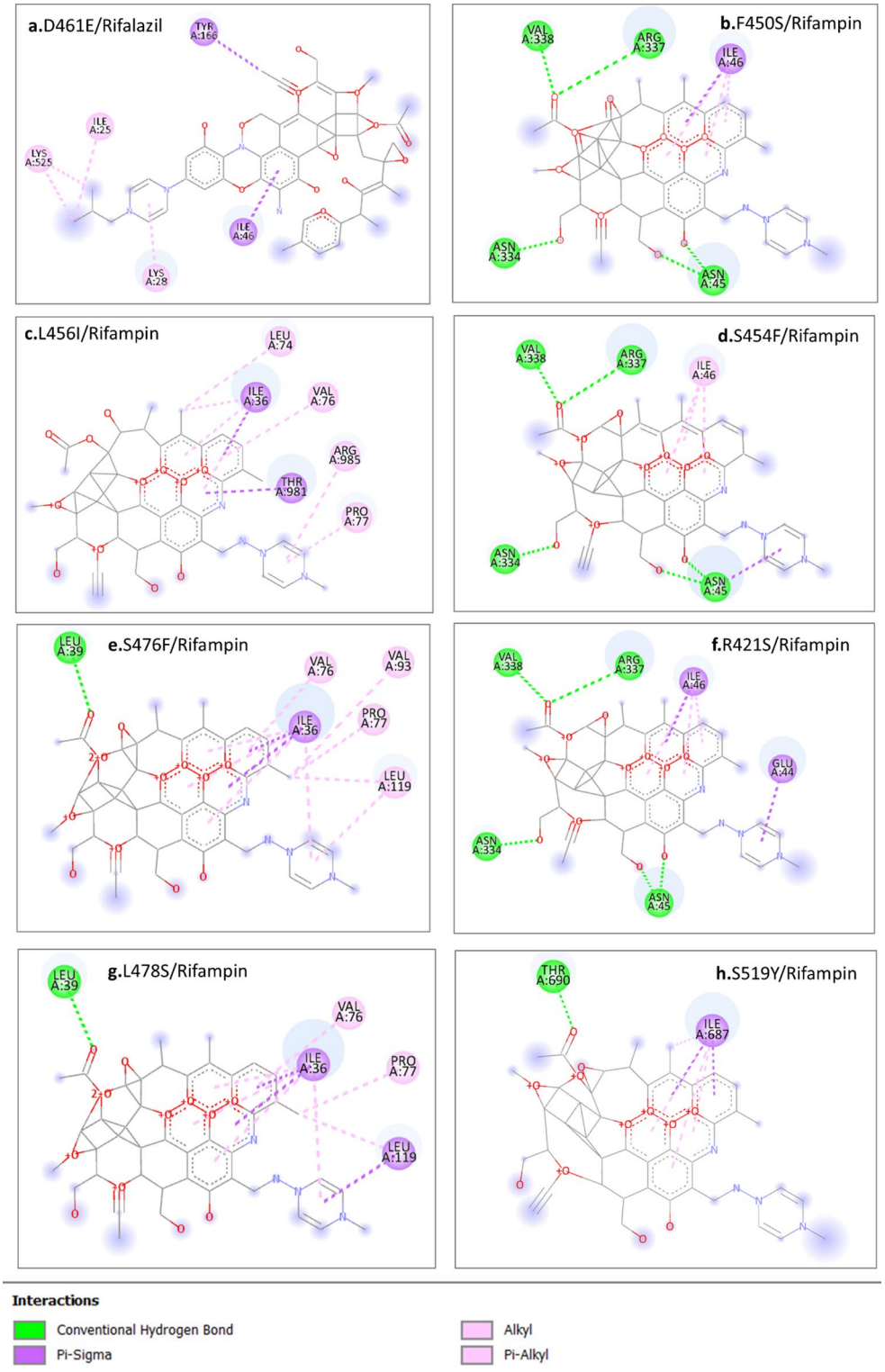

Fig. 7 2D representations of interactions between mutant models of *rpoB*-encoded protein and rifalazil and rifampin

indicate that mutations influence the binding affinity and interaction patterns of rifalazil and rifampin, providing valuable insights into potential mechanisms of antibiotic resistance. The comparable binding energies observed between the wild-type and mutant proteins suggest that the overall energy landscape of ligand binding is not significantly altered due to these mutations (Fig. 6,). However, the changes in interaction patterns indicate

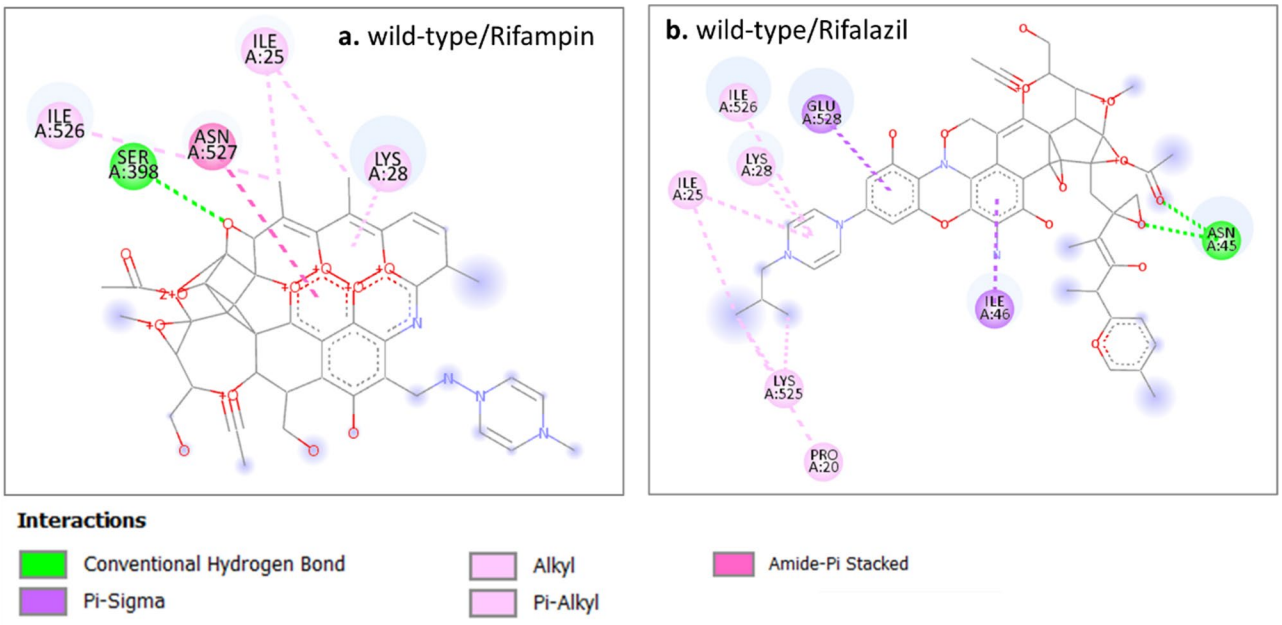

Fig. 8 2D docking interaction representations of the wild-type *rpoB* -encoded protein with rifampin (**a**) and rifalazil (**b**)

Table 9 Prediction of the molecular interactions of the *rpoB*-encoded protein with other proteins via the STRING server

Protein	Description	Score
RpoC	DNA-directed RNA polymerase, beta' subunit; DNA-dependent RNA polymerase catalyzes the transcription of DNA into RNA using the four ribonucleoside triphosphates as substrates.	0.999
RpoA	DNA-directed RNA polymerase, alpha subunit; DNA-dependent RNA polymerase catalyzes the transcription of DNA into RNA using the four ribonucleoside triphosphates as substrates.	0.998
RplK	Ribosomal protein L11; Forms part of the ribosomal stalk, which helps the ribosome interact with GTP-bound translation factors.	0.993
RplF	Ribosomal protein L6 binds to the 23 S rRNA and is essential in its secondary structure. It is located near the subunit interface in the base of the L7/L12 stalk and the tRNA binding site of the peptidyltransferase center; it Belongs to the universal ribosomal protein uL6 family.	0.992
RplC	Ribosomal protein L3: One of the primary rRNA binding proteins, it binds directly near the 3'-end of the 23 S rRNA, where it nucleates the assembly of the 50 S subunit and belongs to the universal ribosomal protein uL3 family.	0.989
RplV	Ribosomal protein L22 binds specifically to 23 S rRNA; its binding is stimulated by other ribosomal proteins, e.g. L4, L17, and L20. It is important during the early stages of 50 S assembly. It makes multiple contacts with different domains of the 23 S rRNA in the assembled 50 S subunit and ribosome (By similarity).	0.987
RplJ	Ribosomal protein L10; Forms part of the ribosomal stalk, playing a central role in the interaction of the ribosome with GTP-bound translation factors. Belongs to the universal ribosomal protein uL10 family.	0.984
RpsE	Ribosomal protein S5, With S4 and S12, plays an essential role in translational accuracy and belongs to the universal ribosomal protein uS5 family.	0.983
RplL	Ribosomal protein L7/L12 Forms part of the ribosomal stalk, which helps the ribosome interact with GTP-bound translation factors. It is thus essential for accurate translation; it Belongs to the bacterial ribosomal protein bL12 family.	0.983
RpsC	Ribosomal protein S3; Binds the lower part of the 30 S subunit head. Binds mRNA in the 70 S ribosome, positioning it for translation; Belongs to the universal ribosomal protein uS3 family.	0.982

structural modifications within the binding pocket that could impact ligand efficacy (Table 8) and (Figs. 7 and 8). In the wild-type protein, rifalazil establishes a strong hydrogen bond with ASN:45, which is likely critical for its binding stability. In mutant forms, rifalazil loses this capability to form a hydrogen bond (as evidenced in D461E) and instead depends solely on hydrophobic interactions (Table 8). This reduction in polar interactions may compromise rifalazil effectiveness, and facilitate the development of antibiotic resistance. Rifampin exhibits fewer interactions within the wild-type protein, suggesting a weaker baseline affinity in comparison to rifalazil (Fig. 6) and (Table 8). However, in certain mutants, such as F450S and R421S, rifampin acquires additional hydrogen bonds (for instance, with ASN:45 and ARG:337), which may enhance its binding stability (Table 8). Conversely, other mutants like S476F and L456I exhibit diminished hydrogen bonding capabilities, resulting in a shift in rifampin interactions towards hydrophobic residues, which may reduce its overall effectiveness

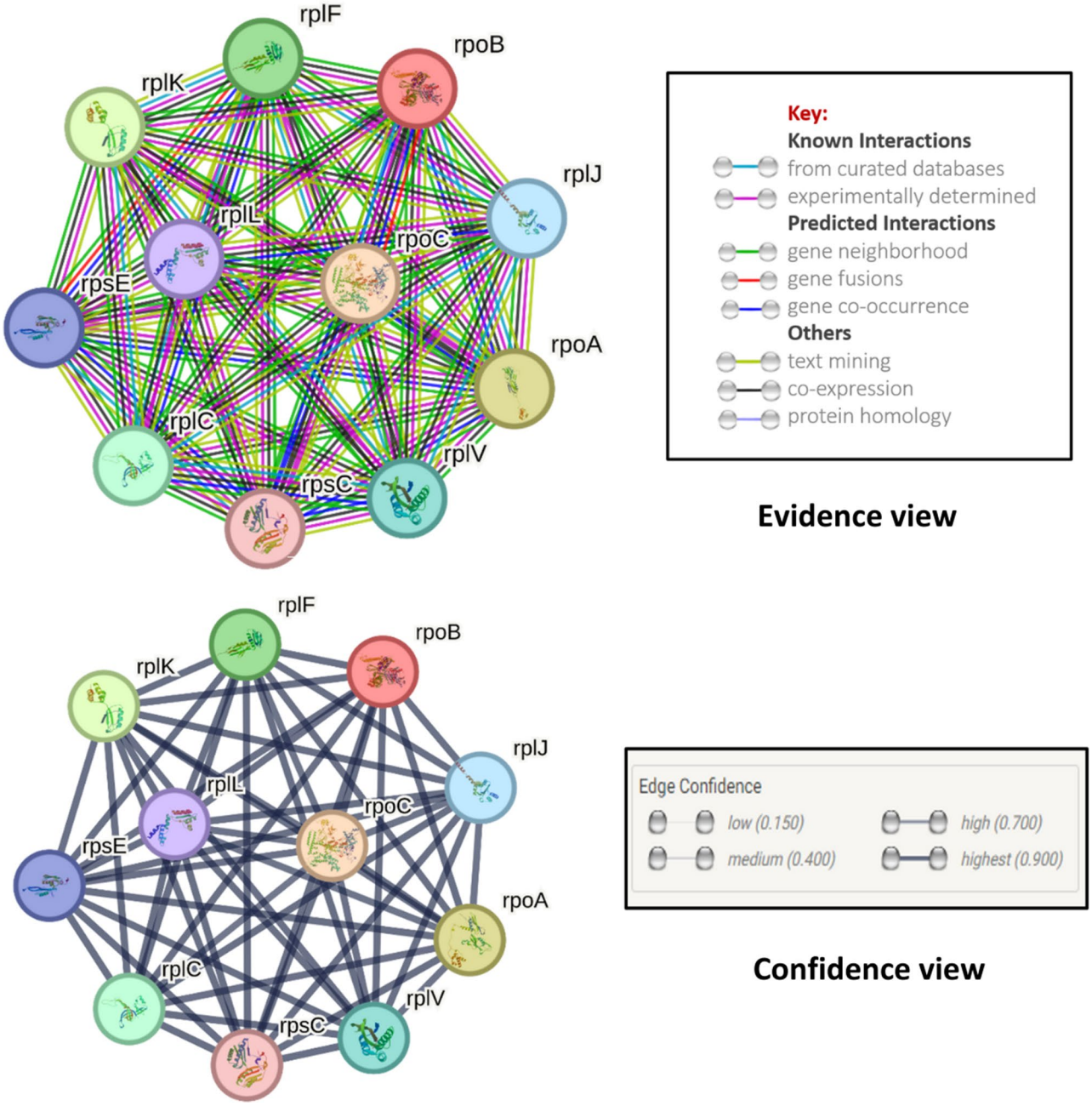

Fig. 9 Overview of *rpoB*-encoded protein network construction via the STRING server. The evidence view and confidence view are given

(Table 8). Mutations that decrease hydrogen bonding—such as D461E for rifalazil and S476F for rifampin—alter the interaction profile and may subsequently reduce the binding stability of these antibiotics. In contrast, mutations like F450S and R421S, which enhance rifampin hydrogen bonding, may allow for compensation of structural changes and enable the protein to adapt, contributing to partial resistance. Finally, the prediction of protein-protein interactions revealed that the *rpoB*-encoded protein interacts with 10 different bacterial proteins (Fig. 9). These proteins are essential for ribosome function and RNA polymerase activity (Table 9). The interactions between the *rpoB*-encoded protein and the RNA polymerase subunits (*RpoC* and *RpoA*) underscore the central role of *rpoB* in transcription—a process targeted by antibiotics such as rifampin and rifalazil. Mutations in the *rpoB* gene can disrupt these interactions, potentially altering the structure or function of the RNA polymerase complex. Such alterations may result in reduced sensitivity or even resistance to transcription-inhibiting antibiotics. Furthermore, the interactions of *rpoB*-encoded protein with ribosomal proteins highlight

the interconnected nature of transcription and translation, both of which are essential for bacterial survival. Ribosomal proteins like *RplC*, *RplF*, and *RpsE* are known targets for antibiotics, including macrolides and aminoglycosides. These findings suggest that any changes to the *rpoB*-encoded protein might impact its interactions with these partners and the complex network of molecular activities supporting cellular function. Importantly, some of these tools have inherent errors and biases, such as algorithmic limitations, reliance on potentially outdated or incomplete databases, and an inability to fully capture the complexities of gene expression and interactions.

Conclusion

This study used various bioinformatics tools to assess the mutations in the *rpoB*-encoded protein associated with *C. pneumoniae's* resistance to rifampin or rifalazil. The impact of the mutations on function, stability, structure, antibiotic binding and interaction was analysed, considering their location in highly conserved regions. These mutations can affect protein function, structure, and interactions, explaining the observed antibiotic resistance. However, not all mutations result in severe functional impacts. Therefore, the information obtained from this in silico analysis can serve as a valuable resource for further exploration into the mechanisms of *C. pneumoniae* resistance, ultimately assisting in the management of infections and the prevention of complications.

Abbreviations

C	Chlamydia
ΔG	Gibbs free energy of unfolding
ΔΔG	Change in Gibbs free energy of unfolding
RMSD	Root means square deviation
rpoB	RNA polymerase β-subunit gene

Acknowledgements

Sanae Esskhayry gratefully acknowledges the support of the CNRST (National Centre for Scientific and Technical Research) in Morocco for the PhD Associate Scholarship PASS.

Author contributions

SE: Data extraction, data curation, data analysis, study design, and drafting of the paper. IB: study design and data analysis. FR: Project conception, Study design, Following the study process, Validating the data, and drafting and validating the paper. OK: drafting and revising the paper. AL, RF, and AM: revising the paper. All the authors read and approved the manuscript.

Funding

Not applicable.

Data availability

No datasets were generated or analysed during the current study.

Declarations

Ethics approval and consent to participate

Not applicable.

Consent for publication

Not applicable.

Competing interests

The authors declare no competing interests.

Author details

[1]Life and Health Sciences Laboratory, Faculty of Medicine and Pharmacy, Abdelmalek Essaâdi University, Tangier, Morocco
[2]Department of Medical Genetics and Oncogenetics, Mohammed VI University Hospital Center, Tangier, Morocco
[3]Systems and Data Engineering Team, National School of Applied Sciences, Abdelmalek Essaâdi University, Tangier 90 000, Morocco
[4]Laboratory of Information Technology and Modeling, Faculty of Sciences Ben M'Sik, Hassan II University of Casablanca, B. P 7955 Sidi Othmane, Casablanca, Morocco
[5]Chlamydiae and Mycoplasma Laboratory, Research Department, Institut Pasteur du Maroc, Casablanca 20360, Morocco

Received: 20 September 2024 / Accepted: 3 March 2025
Published online: 19 March 2025

References

1. Bachmann NL, Polkinghorne A, Timms P. Chlamydia genomics: providing novel insights into chlamydial biology. Trends Microbiol. 2014;22(8):464–72. https://doi.org/10.1016/j.tim.2014.04.013.
2. Nunes A, Gomes JP. Evolution, phylogeny, and molecular epidemiology of Chlamydia. Infect Genet Evol. 2014;23:49–64. https://doi.org/10.1016/j.meegid.2014.01.029.
3. Vorimore F, Hölzer M, Liebler-Tenorio EM, Barf L-M., Delannoy S, Vittecoq M, et al. Evidence for the existence of a new genus Chlamydiifrater gen. nov. inside the family Chlamydiaceae with two new species isolated from flamingo (Phoenicopterus roseus): Chlamydiifrater phoenicopteri sp. nov. and Chlamydiifrater volucris sp. nov. Systematic and Applied Microbiology. 2021 Mar 30;44(4):126200. https://doi.org/10.1016/j.syapm.2021.126200
4. Hammerschlag MR, Kohlhoff SA, Gaydos CA. Chlamydia pneumoniae. In: Bennett JE, Dolin R, Blaser MJ, editors. Mandell, Douglas, and Bennett's principles and practice of infectious diseases. 8th ed. Philadelphia: Elsevier; 2015. pp. 2174–e21822. https://doi.org/10.1016/B978-1-4557-4801-3.00184-3
5. Sandoz KM, Rockey DD. Antibiotic resistance in Chlamydiae. Future Microbiol. 2010;5(9):1427–42. https://doi.org/10.2217/fmb.10.96.
6. Llor C, Bjerrum L. Antimicrobial resistance: risk associated with antibiotic overuse and initiatives to reduce the problem. Ther Adv Drug Saf. 2014;5(6):229–41. https://doi.org/10.1177/2042098614554919.
7. Uddin TM, Chakraborty AJ, Khusro A, Zidan BRM, Mitra S, Emran TB, et al. Antibiotic resistance in microbes: History, mechanisms, therapeutic strategies and future prospects. Journal of Infection and Public Health. 2021 Oct 25;14(12):1750–66. https://doi.org/10.1016/j.jiph.2021.10.020
8. Ventola CL. The antibiotic resistance crisis. P T. 2015;40(4):277–83.
9. Murray CJL, Ikuta KS, Sharara F, Swetschinski L, Aguilar GR, Gray A, et al. Global burden of bacterial antimicrobial resistance in 2019: a systematic analysis. The Lancet. 2022 Jan 19;399(10325):629–55.
10. Tenover FC. Mechanisms of antimicrobial resistance in Bacteria. Am J Med. 2006;119(6 Suppl 1). https://doi.org/10.1016/j.amjmed.2006.03.011.
11. Benamri I, Azzouzi M, Sanak K, Moussa A, Radouani F. An overview of genes and mutations associated with Chlamydiae species' resistance to antibiotics. Ann Clin Microbiol Antimicrob. 2021;20(1):59. https://doi.org/10.1186/s12941-021-00465-4.
12. Kutlin A, Kohlhoff S, Roblin P, Hammerschlag MR, Riska P. Emergence of resistance to Rifampin and Rifalazil in Chlamydophila pneumoniae and *Chlamydia trachomatis*. Antimicrob Agents Chemother. 2005;49(3):903–7. https://doi.org/10.1128/AAC.49.3.903-907.2005.
13. Rothstein DM, Suchland RJ, Xia M, Murphy CK, Stamm WE. Rifalazil retains activity against rifampin-resistant mutants of *Chlamydia pneumoniae*. J Antibiot (Tokyo). 2008;61(8):489–95. https://doi.org/10.1038/ja.2008.65
14. Michalovich D, Overington J, Fagan R. Protein sequence analysis in Silico: application of structure-based bioinformatics to genomic initiatives. Curr Opin Pharmacol. 2002;2(5):574–80. https://doi.org/10.1016/S1471-4892(02)00202-3.
15. Kucukkal TG, Petukh M, Li L, Alexov E. Structural and physicochemical effects of disease and nondisease NsSNPs on proteins. Curr Opin Struct Biol. 2015;32:18–24. https://doi.org/10.1016/j.sbi.2015.01.003.

16. Benamri I, Azzouzi M, Moussa A, Radouani F. An in Silico analysis of RpoB mutations to affect *Chlamydia trachomatis* sensitivity to rifamycin. J Genet Eng Biotechnol. 2022;20(1):146. https://doi.org/10.1186/s43141-022-00428-y.
17. Varadi M, Bertoni D, Magana P, Paramval U, Pidruchna I, Radhakrishnan M, et al. AlphaFold Protein Structure Database in 2024: providing structure coverage for over 214 million protein sequences. Nucleic Acids Research. 2023 Nov 2;52(D1):D368–75. https://doi.org/10.1093/nar/gkad1011
18. Pejaver V, Urresti J, Lugo-Martinez J, Pagel KA, Lin GN, Nam HJ, et al. Inferring the molecular and phenotypic impact of amino acid variants with MutPred2. Nature Communications. 2020 Nov 20;11(1). https://doi.org/10.1038/s41467-020-19669-x
19. Bendl J, Stourac J, Salanda O, Pavelka A, Wieben ED, Zendulka J, et al. PredictSNP: Robust and Accurate Consensus Classifier for Prediction of Disease-Related Mutations. PLoS Computational Biology. 2014 Jan 16;10(1):e1003440. https://doi.org/10.1371/journal.pcbi.1003440
20. Ng PC, Henikoff S. SIFT: predicting amino acid changes that affect protein function. Nucleic Acids Res. 2003;31(13):3812–4. https://doi.org/10.1093/nar/gkg509.
21. Ramensky V, Bork P, Sunyaev S. Human non-synonymous SNPs: server and survey. Nucleic Acids Res. 2002;30(17):3894–900. https://doi.org/10.1093/nar/gkf493.
22. Adzhubei I, Jordan DM, Sunyaev SR. Predicting functional effect of human missense mutations using PolyPhen-2. Curr Protoc Hum Genet. 2013;76(1):7–20. https://doi.org/10.1002/0471142905.hg0720s76.
23. Stone EA, Sidow A. Physicochemical constraint violation by missense substitutions mediates impairment of protein function and disease severity. Genome Res. 2005;15(7):978–86. https://doi.org/10.1101/gr.3804205.
24. Capriotti E, Calabrese R, Casadio R. Predicting the insurgence of human genetic diseases associated to single point protein mutations with support vector machines and evolutionary information. Bioinformatics. 2006;22(22):2729–34. https://doi.org/10.1093/bioinformatics/btl423.
25. Bromberg Y, Rost B. SNAP: predict effect of non-synonymous polymorphisms on function. Nucleic Acids Res. 2007;35(11):3823–35. https://doi.org/10.1093/nar/gkm238.
26. Tang H, Thomas PD. PANTHER-PSEP: predicting disease-causing genetic variants using position-specific evolutionary preservation. Bioinformatics. 2016;32(14):2230–2. https://doi.org/10.1093/bioinformatics/btw222.
27. Cheng J, Randall A, Baldi P. Prediction of protein stability changes for single-site mutations using support vector machines. Proteins. 2006;62(4):1125–32. https://doi.org/10.1002/prot.20810.
28. Bao L, Zhou M, Cui Y. NsSNPAnalyzer: identifying disease-associated nonsynonymous single nucleotide polymorphisms. Nucleic Acids Res. 2005;W480–2. https://doi.org/10.1093/nar/gki372. 33(Web Server issue).
29. Sanavia T, Birolo G, Montanucci L, Turina P, Capriotti E, Fariselli P. Limitations and challenges in protein stability prediction upon genome variations: towards future applications in precision medicine. Computational and Structural Biotechnology Journal. 2020 Jan 1;18:1968–79. https://doi.org/10.1016/j.csbj.2020.07.011
30. Pancotti C, Benevenuta S, Birolo G, Alberini V, Repetto V, Sanavia T, et al. Predicting protein stability changes upon single-point mutation: a thorough comparison of the available tools on a new dataset. Brief Bioinform. 2022;23(2):bbab555.
31. Rodrigues CHM, Pires DEV, Ascher DB. DynaMut2: assessing changes in stability and flexibility upon single and multiple point missense mutations. Protein Sci Publ Protein Soc. 2021;30(1):60–9.
32. Li G, Panday SK, Alexov E. SAAFEC-SEQ: A Sequence-Based method for predicting the effect of single point mutations on protein thermodynamic stability. Int J Mol Sci. 2021;22(2):606.
33. Ashkenazy H, Abadi S, Martz E, Chay O, Mayrose I, Pupko T, et al. ConSurf 2016: an improved methodology to estimate and visualize evolutionary conservation in macromolecules. Nucleic Acids Research. 2016 May 10;44(W1):W344–50. https://doi.org/10.1093/nar/gkw408
34. Goldenberg O, Erez E, Nimrod G, Ben-Tal N. The ConSurf-DB: precalculated evolutionary conservation profiles of protein structures. Nucleic Acids Res. 2009;37(Database issue). https://doi.org/10.1093/nar/gkn822.
35. Ashkenazy H, Erez E, Martz E, Pupko T, Ben-Tal N. ConSurf 2010: calculating evolutionary conservation in sequence and structure of proteins and nucleic acids. Nucleic Acids Res. 2010;38(Web Server issue). https://doi.org/10.1093/nar/gkq399.
36. Pace CN, Fu H, Fryar KL, Landua J, Trevino SR, Schell D, et al. Contribution of hydrogen bonds to protein stability. Protein Sci Publ Protein Soc. 2014;23(5):652–61. https://doi.org/10.1002/pro.2449.
37. Guex N, Peitsch MC. SWISS-MODEL and the Swiss-PdbViewer: an environment for comparative protein modelling. Electrophoresis. 1997;18(15):2714–23. https://doi.org/10.1002/elps.1150181505.
38. Waterhouse A, Bertoni M, Bienert S, Studer G, Tauriello G, Gumienny R, et al. SWISS-MODEL: homology modelling of protein structures and complexes. Nucleic Acids Res. 2018;46(W1):W296–303. https://doi.org/10.1093/nar/gky427.
39. Williams CJ, Headd JJ, Moriarty NW, Prisant MG, Videau LL, Deis LN, et al. MolProbity: More and better reference data for improved all-atom structure validation. Protein Science. 2017 Oct 25;27(1):293–315. https://doi.org/10.1002/pro.3330
40. Pettersen EF, Goddard TD, Huang CC, Couch GS, Greenblatt DM, Meng EC, et al. UCSF Chimera–a visualization system for exploratory research and analysis. J Comput Chem. 2004;25(13):1605–12. https://doi.org/10.1002/jcc.20084.
41. Kini RM, Evans HJ. Molecular modelling of proteins: a strategy for energy minimization by molecular mechanics in the AMBER force field. J Biomol Struct Dyn. 1991;9(3):475–88. https://doi.org/10.1080/07391102.1991.10507930.
42. Suvethigaa S, Chomilier J, Carpentier M. Structural effects of point mutations in proteins. Proteins. 2018;86(8):853–67. https://doi.org/10.1002/PROT.25499.
43. Ramanathan K. A systematic review on molecular Docking algorithms and its challenges. Int J Pharm Sci Rev Res. 2016;36(1):148–56.
44. Bitencourt-Ferreira G, Pintro VO, de Azevedo WF Jr. Docking with AutoDock4. Methods Mol Biol. 2019;2053:125–48. https://doi.org/10.1007/978-1-4939-9752-7_9.
45. Xu Y, Wang S, Hu Q, Gao S, Ma X, Zhang W, et al. CavityPlus: a web server for protein cavity detection with pharmacophore modelling, allosteric site identification and covalent ligand binding ability prediction. Nucleic Acids Research. 2018 Apr 30;46(W1):W374–9. https://doi.org/10.1093/nar/gky380
46. Sakhawat A, Khan MU, Rehman R, Khan S, Shan MA, Batool A, et al. Natural compound targeting BDNF V66M variant: insights from in silico docking and molecular analysis. AMB Express. 2023 Nov 28;13(1). https://doi.org/10.1186/s13568-023-01640-w
47. Farooq QA, Shaukat Z, Aiman S, Li CH. Protein–protein interactions: methods, databases, and applications in virus–host study. World J Virol. 2021;10(6):288–300. https://doi.org/10.5501/wjv.v10.i6.288.
48. Szklarczyk D, Gable AL, Lyon D, Junge A, Wyder S, Huerta-Cepas J, et al. STRING v11: protein–protein association networks with increased coverage, supporting functional discovery in genome-wide experimental datasets. Nucleic Acids Research. 2018 Nov 17;47(D1):D607–13. https://doi.org/10.1093/nar/gky1131
49. Kutlin A, Roblin PM, Hammerschlag MR. Effect of prolonged treatment with Azithromycin, clarithromycin, or Levofloxacin on *Chlamydia pneumoniae* in a Continuous-Infection model. Antimicrob Agents Chemother. 2002;46(2):409–12. https://doi.org/10.1128/AAC.46.2.409-412.2002
50. Ameyama S, Shinmura Y, Takahata M. Inhibitory activities of quinolones against DNA gyrase of *Chlamydia pneumoniae*. Antimicrob Agents Chemother. 2003;47(7):2327–9. https://doi.org/10.1128/AAC.47.7.2327-2329.2003
51. Hammerschlag MR. Activity of Gemifloxacin and other new quinolones against *Chlamydia pneumoniae*: a review. J Antimicrob Chemother. 2000;45(suppl3):35. https://doi.org/10.1093/jac/45.suppl_3.35
52. Patini R, Mangino G, Martellacci L, Quaranta G, Masucci L, Gallenzi P. The effect of different antibiotic regimens on bacterial resistance: a systematic review. Antibiotics. 2020 Jan 8;9(1):22. https://doi.org/10.3390/antibiotics9010022
53. Mahmood RK, Gillani SW, Alzaabi MJ, Gulam SM. Evaluation of inappropriate antibiotic prescribing and management through pharmacist-led antimicrobial stewardship programmes: a meta-analysis of evidence. Eur J Hosp Pharm. 2022;29(1):2–7. https://doi.org/10.1136/ejhpharm-2021-002914.
54. Sulis G, Daniels B, Kwan A, Gandra S, Daftary A, Das J, et al. Antibiotic overuse in the primary health care setting: a secondary data analysis of standardised patient studies from India, China and Kenya. BMJ Global Health. 2020 Sep 1;5(9):e003393. https://doi.org/10.1136/bmjgh-2020-003393

Publisher's note